THE JOURNAL OF
Obstetrics and Gynaecology Research

doi:10.1111/jog.14495 J. Obstet. Gynaecol. Res. Vol. 46, No. 12: 2561–2572, December 2020

Exosomal microRNA-139-5p from mesenchymal stem cells accelerates trophoblast cell invasion and migration by motivation of the ERK/MMP-2 pathway via downregulation of protein tyrosine phosphatase

Huijie Liu[1], Fang Wang[2], Ying Zhang[3], Yanling Xing[3] and Qian Wang[4]

[1]*Department of Obstetrics, Liaocheng Second People's Hospital, Liaocheng, Shandong, China*
[2]*Department of Obstetrics and Gynecology, Jinxiang People's Hospital, Jining, Shandong, China*
[3]*Department of Obstetrics and Gynecology, Chiping People's Hospital, Liaocheng, Shandong, China*
[4]*Department of Obstetrics, Weifang Maternal and Child Health Hospital, Weifang, Shandong, China*

Abstract

Aim: Exosomes present essential roles for intercellular interaction via extracellular pathways during systemic dysfunctions, including preeclampsia (PE). Here, we assessed the specific mechanism of mesenchymal stem cells (MSC)-originated exosomes in PE.

Methods: The effects of exosomes on trophoblasts were studied by EdU, wound healing, Transwell and TUNEL assays. By microarray analysis, we found that exosomes enhanced the microRNA-139-5p (miR-139-5p) in trophoblasts, and confirmed the target gene of miR-139-5p by bioinformatics prediction and dual-luciferase reporter gene assay. At the same time, ERK/MMP-2 pathway-related biomolecules were assessed through Western blot analysis. The pathway inhibitor was used for rescue experiments. Finally, the effect of exosomes on the pathology of PE rats was verified by *in vivo* experiments.

Results: The exosomes originated from hucMSC fostered the trophoblast cell migration, invasion and proliferation and obstructed apoptosis. Moreover, miR-139-5p could be transmitted to trophoblasts through hucMSC-secreted exosomes. miR-139-5p targeted protein tyrosine phosphatase (PTEN), which regulated the ERK/MMP-2 pathway. Inhibition of the ERK/MMP-2 pathway significantly reduced the promoting effect of exosomes on trophoblasts. Treatment with exosomes significantly lowered blood pressure values and reduced 24-h proteinuria in PE rats.

Conclusion: hucMSC-originated exosomes overexpressing miR-139-5p activated the ERK/MMP-2 pathway via PTEN downregulation, thus accelerating trophoblast cell invasion and migration, and blocking apoptosis. These results demonstrated that hucMSC-derived exosomes overexpressing miR-139-5p might be an innovative direction for therapeutic approaches against PE.

Key words: ERK/MMP-2, exosomes, human umbilical mesenchymal stem cells, microRNA-139-5p, preeclampsia, PTEN.

Introduction

Preeclampsia (PE) is described as a systemic disease depicted by the new onset of elevated blood pressure over 140/90 mm Hg and proteinuria after gestation in a formerly normotensive female for 20 weeks.[1] The incidence rate of pregnancy-induced hypertension syndrome is one of the principal causes of maternal

Received: May 21 2020.
Accepted: September 5 2020.
Correspondence: Ms. Qian Wang, Department of Obstetrics, Weifang Maternal and Child Health Hospital, No. 76, Qingnian Road, Weicheng District, Weifang 261000, Shandong, China. Email: qianwang010603@163.com

morbidity and perinatal mortality, which accounts for 3–5% of whole pregnancies.[2] PE affects about 76 000 pregnant females every year, resulting in 500 000 infant mortalities globally.[3] Different factors are considered to be risk reasons for PE such as age, renal disease, chronic hypertension, diabetes mellitus and obesity.[4] PE is generally considered to be the result of the placental failure, which is categorized by the irregular remodeling of the spiral artery due to the invasion of superficial trophoblasts.[5] As delivery is the only effective way for curing the disease, treatment is mainly concentrated on the management of blood pressure and other clinical manifestations.[6]

Successful isolation of mesenchymal stem cells (MSC) from the placental decidua basalis tissue of human PE was reported by Yasser S. Basmaeil *et al*.[7] Furthermore, the exosomes emitted by MSC encompass the curative capacity to hinder apoptosis and stimulate angiogenesis in the placenta.[8] Interestingly, around 60% of the circulating microRNAs (miRNA) is linked with exosomes, and the miRNA in exosomes are resilient to RNase management.[9] miRNA play an essential role in placental-related disorders by binding to the 3′-untranslated region of target mRNA, thus hindering the expression of target mRNA.[10] microRNA-139-5p (miR-139-5p) is positioned in the human chromosome 11q13.4 region,[11] which has been recognized as a tumor-conquering miRNA due to its downregulation in numerous types of tumor, such as non-small cell lung, prostate and breast cancers.[12–14] Interestingly, a study uncovered the function of miR-139-5p in trophoblasts by regulating soluble fms-like tyrosine kinase-1 in PE.[15] Moreover, decreased exosomal miR-139-3p expression in plasma of the patients with colorectal cancer has the potency to serve as a novel biomarker for the early diagnosis and metastasis monitoring.[16] Recently, more and more studies have examined the importance of circulating exosomes in PE.[17,18] However, there are few studies at present to evaluate the specific mechanism of miRNA in MSC-derived exosomes.

This study is intended to search the difference of exosomal miRNA expression in PE to further examine the latent mechanism of exosomal encapsulated miR-139-5p in both trophoblasts and rats with PE. This exploration could initiate uncovering a novel biomarker for the early diagnosis of PE and a new understanding of PE pathogenesis.

Methods

Cell culture

Human umbilical cord MSC (hucMSC) and HTR-8/Svneo cells were bought from American Type Culture Collection (Manassas, VA, USA). The cells were cultured in Dulbecco's modified Eagle's medium (DMEM) comprising penicillin-streptomycin (100 U/mL, Gibco Life Technologies) and 10% fetal bovine serum (FBS) (Biowest) in an incubator (37°C, 5% CO_2). The methods and results for hucMSC identification are presented in the Supplementary Material.

Extraction and verification of hucMSC-produced exosomes

Exosomes were removed from the serum-containing medium by overnight ultracentrifugation at 100 000*g* at 4°C. The hucMSC were incubated in DMEM overnight. When cell confluence reached approximately 80–90%, hucMSC were further incubated in exosome-free serum medium for 24 h, and then the supernatant was collected. The cells were centrifuged at 2000 g at 4°C for 20 min to remove cell debris, and the supernatant obtained was centrifuged at 10 000*g* at 4°C for 1 h. The precipitate was then suspended in serum-free DMEM containing 25 mM n-2-hydroxyethylpiperazine-n′-2-ethanesulfonic Acid (pH = 7.4) to repeat the ultracentrifugation. The precipitate was then stored at −80°C for later use.[19] As reported previously,[20] the identification of exosomes is described in the Supplementary Material.

Fluorescent labeling of exosomes

The exosomes isolated from MSC were marked with PKH26 (Red, MINI26-1KT; Sigma). Then, exosomes trailed by PKH26 were cultured with HTR-8/Svneo cells with 50–60% confluence for 48 h in a 24-well plate, and Hoechst 33342 (MedChemExpress) was adopted to stain cell nuclei. The cells were perceived under an inverted fluorescence microscope (NuoHaiLifeScience).

Cell transfection

The plasmids miR-139-5p mimic/inhibitor and its negative control (NC) were from GenePharma Co., Ltd. The specific transfection procedure is listed in the Supplementary Material. Extracellular regulated protein kinases (ERK)1/2 inhibitor, the inhibitor of the ERK/matrix metalloproteinase-2 (MMP-2) pathway, was purchased from MedChemExpress (HY-112287). The ERK1/2 inhibitor used for HTR-8/Svneo

treatment was 2 μmol/L, while the exosome concentration was 40 μg/mL.

Cell proliferation tests

5-Ethynyl-2′-deoxyuridine (EdU) imaging test kit (Thermo Fisher Scientific) was used for EdU staining. EdU staining solution was added to each well 48 h after transfection and incubated at 37°C for 2 h. The cells were fixed in 4% paraformaldehyde for 15 min and incubated with phosphate buffered saline (PBS) containing 0.5% Triton X-100 for 20 min. Then, the cells were incubated with Click-iT reaction solution for 30 min in the dark room and stained with Hoechst 33342. Cells were observed by fluorescence microscopy (Olympus), and the positive rate was calculated by ImageJ.

For cell counting kit-8 (CCK-8) assay, the cells were positioned in a 96-well plate (3×10^3 cells/well), and then cultured for 24, 48 or 72 h. Next, the CCK8 solution (Yeasen) was added, and the cells were incubated at 37°C for another 2 h. The optical density (OD) value (450 nm) was measured with a spectrophotometer (Thermo Fisher Scientific).

Wound healing assay

A wound-healing assay was executed to assess the cell migratory ability of HTR-8/SVneo cells. A wound of about 1 mm width was created by scraping the monolayer in the center of the well using a 10-μL pipette tip. The migration distance was detected after scratching of 0, 24 and 48 h and photographed. The cell-free area was calculated by IPP7.0 software, and the area was compared with that at the 0 h to estimate the migration rate.

Transwell assay

Cell suspension (100 μL) in serum-free medium (1×10^5 cells/mL) was loaded into the apical chamber of cell culture inserts (8 μm pore size, 24-well; BD Biosciences) pre-covered with Matrigel (BD Biosciences) membrane. Roswell Park Memorial Institute-1640 medium (600 μL) encompassing 10% FBS was supplemented to the basolateral chamber as chemo-attractant. After 24 h of incubation at 37°C, cells invaded through the membrane were dyed with 0.1% crystal violet at room temperature (20°C) for 20 min. The invasive cells were calculated under a microscope (Nikon E100; Nikon Corp, Japan) and averaged from five random fields.

Enzyme linked immunosorbent assay (ELISA)

The effect of exosome treatment on the expression of Cleaved-caspase-3 (c-caspase-3) in trophoblasts was determined by using human c-caspase-3 (Asp175) ELISA kit (ab220655, Abcam Inc.).

Cell apoptosis tests

Terminal deoxyribonucleotidyl transferase (TDT)-mediated 2′-Deoxyuridine 5′-Triphosphate (dUTP) nick end-labeling (TUNEL) reaction mixture was prepared using a TUNEL kit (green fluorescence, C1088, Beyotime). Fluorescein labeled dUTP and/or TDT solution was added to the cells devoid of light at 37°C for 60 min. The cells were sealed with an anti-fluorescence quenching solution and observed under a fluorescence microscope with 450 nm excitation wavelength and 550 nm emission wavelength (green fluorescence).

For flow cytometry of cell apoptosis, the Annexin V-fluorescein isothiocyanate (FITC) kit of BestBio was used to measure cell apoptosis. Cells were resuspended in 1× binding buffer at 1×10^5 cells/mL and incubated with the mixture of 5 μL FITC/Annexin-V and 5 μL PI in the dark for 15 min. After the addition of 400 μL 1× binding buffer, Cell-Quest software and FACS Calibur (Becton Dickinson) was used to analyze cell apoptosis.

Reverse transcription-quantitative PCR (RT-qPCR)

Trizol reagent (Invitrogen) was used to obtain total RNA. The PrimeScript RT Kit (Takara) or TaqMan miRNA RT Kit (4366596) was used for reverse transcription. SYBR Premier Ex Taq kit (RR820A, Takara) was utilized to carry out RT-qPCR on ABI 7500 system (Thermo Fisher Scientific). Glyceraldehyde-3-phosphate dehydrogenase (GAPDH) was the internal parameter of protein tyrosine phosphatase (PTEN), U6 was the internal parameter of miR-139-5p. The $2^{-\Delta\Delta Ct}$ method was used to determine fold changes. The primer sequences are list in Table 1.

Microarray analysis

TRIzol Reagent (Invitrogen) was used to obtain total RNA, which was then purified by an RNeasy Mini Kit (Qiagen). rtStar PreAMP cDNA kit was adopted to synthesize and pre-amplify cDNA. Then, the cDNA was marked and hybridized with the miRNA Expression Microarray (Arraystar). After washing, slides were examined on the miRs microarray. Using

Table 1 The primer sequences for RT-qPCR

Gene	Primer sequence
hsa-miR-139-5p	F: 5′-GCCTCTACAGTGCACGTGTCTC-3′ R: 5′-CGCTGTTCTCATCTGTCTCGC-3′
rno-miR-139-5p	F: 5′-ACACTCCAGCTGGGT CTACAGTGCAC-3′ R: 5′-TGGTGTCGTGGAGTCG-3′
hsa-PTEN	F: 5′-GCATGTATTCGGGTTAGG-3′ R: 5′-TGAATGAAACTGACAAGG-3′
rno-PTEN	F: 5′- TGGGAGTAGACGGATGCGAA-3′ R: 5′- AACCAATCCGTGCCTTGACA-3′
rno-MMP2	F: 5′-CCTTGGGGCAGCCATAGAAA-3′ R: 5′-TGTTTGGCAGAAGTTGGGGT-3′
hsa-U6	F: 5′-CTCGCTTCGGCAGCACA-3′ R: 5′-AACGCTTCACGAATTTGCGT-3′
rno-U6	F: 5′-GCTTCGGCAGCA CATATACTAAAAT-3′ R: 5′-CGCTTCACGAATTTGCGTGCAT-3′
hsa-GAPDH	F: 5′-TCTCCTCTGACTTCAACAGCGA-3′ R: 5′-GTCCACCACCCTGTTGCTGT-3′
rno-GAPDH	F: 5′-CATCAACGACCCCTTCATTG-3′ R: 5′-GAAGATGGTGATGGGTTTCC-3′

GAPDH, glyceraldehyde-3-phosphate dehydrogenase; hsa, *Homo sapiens*; miR-139-5p, microRNA-139-5p; MMP, metalloproteinase-2; PTEN, phosphatase and tensin homolog deleted on chromosome 10; rno, *Rattus norvegicus*.

GeneSpring GX v12.1 software package (Agilent Technologies), differentially expressed miRNAs were recognized with thresholds of $P < 0.05$ and fold change ≥2.0.

Dual-luciferase reporter gene assay

PTEN fragment containing the putative miR-139-5p binding site was subcloned into the pmirGLO vector (Promega) and named wild type (WT). Then, the predicted miR-139-5p binding site was mutated to make a mutant (MT). Two reported plasmids were co-transfected with miR-139-5p mimic into HTR-8/Svneo cells, respectively. Forty-eight h after transfection, luciferase activity was measured (Promega).

Western blot analysis

Total protein was obtained by radioimmunoprecipitation assay buffer (C0481, Sigma) and then quantified by bicinchoninic acid assay protein Kit (23 227, Thermo Fisher Scientific). After separation with 10% sodium dodecyl sulfate-polyacrylamide gel electrophoresis, the protein samples were transferred into a membrane. The membrane was incubated overnight at 4°C with appropriate primary antibody and with secondary antibody for 2 h, and stained with electrochemiluminescence. Gel-Pro software analyzed the OD value of each band with GAPDH as the internal reference. The antibodies (Abcam Inc.) included MMP-2 (1:5000, ab92536), phosphor (p)-ERK1/2 (1:1000, ab92536), ERK1/2 (1:10000, ab184699), GAPDH (1:10000, ab181602) and the corresponded secondary goat anti-rabbit IgG H and L (HRP) (1:50000, ab205718).

PE rat model and exosome treatment

Thirty Sprague-Dawley rats (20 female and 10 male) were obtained from the Laboratory Animal Center of Liaocheng Second People's Hospital and kept in a cage with a ratio of one male rat to two females. All rats were housed in a temperature-controlled (23 ± 3°C) room on a 12/12 h light/dark cycle with ad libitum access to chow and drinking water. Experiments involving animals were conducted in strict accordance with the approved animal protocols of the Ethics Review Committee of Liaocheng Second People's Hospital. Rats received possible humane care following regulation issued by the National Institutes of Health guide for the care and use of Laboratory animals (NIH publications No. 8023, revised 1978).

The day that sperm was found in the vagina of female rats and the vaginal plug was dropped was determined to be the first day of pregnancy. Pregnant rats were randomly divided into sham group (n = 5), PE group (n = 5) and PE + exo group (n = 5). The exosome treatment was introduced according to a previous report.[21] Supplementary Material displays specific modeling methods and measurements of blood pressure, 24-h proteinuria in rats. After the blood pressure measurement on day 20, the placenta was rapidly removed from the rat after an intraperitoneal injection of sodium pentobarbital. A small piece of the central maternal surface of the placenta with few blood vessels was cut under direct vision, rinsed with saline and made into a homogenate. The gene expression was detected by RT-qPCR.

Statistical analysis

Statistical analysis was accomplished using SPSS 22.0 (IBM Corp.). Normal distribution and homogeneity of variance were tested. The comparison was carried out between two groups by unpaired *t*-test. Data of single factor between two groups were compared by one-way analysis of variance (ANOVA) followed by Tukey's post hoc test, while data of double factors in multiple groups were compared by two-way ANOVA. While $P < 0.05$ statistical significance was designated.

Results

Characterization of hucMSC and hucMSC-secreted exosomes

After 3 days of seeding, the cells were adherent to the wells. The cells were in a whirlpool or cluster with distinct nuclei, presenting typically spindle-shaped MSC characteristics (Figure S1a). We found that poorly expressed CD45 (4.2%) but highly expressed CD44 (98.5%) and CD90 (92.4%), which was coherent with the biological features of MSC (Figure S1b). After 21 days of osteogenic differentiation, the cells

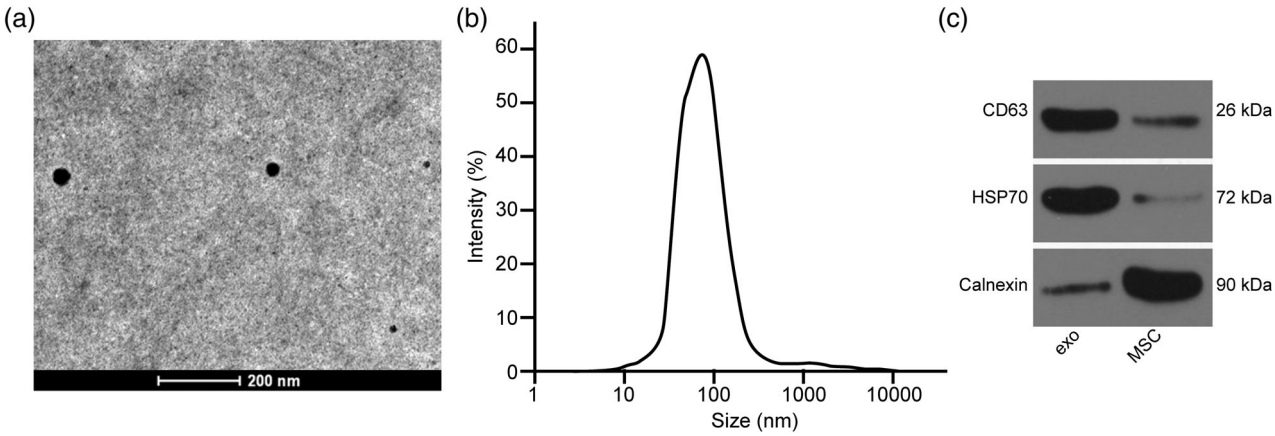

Figure 1 Characterization of MSC-secreted exosomes. (a) Verification of exosomes by a TEM. (b) Detection of exosome distribution by dynamic light scattering. (c) Expression of exosome surface indicators measured by Western blot analysis.

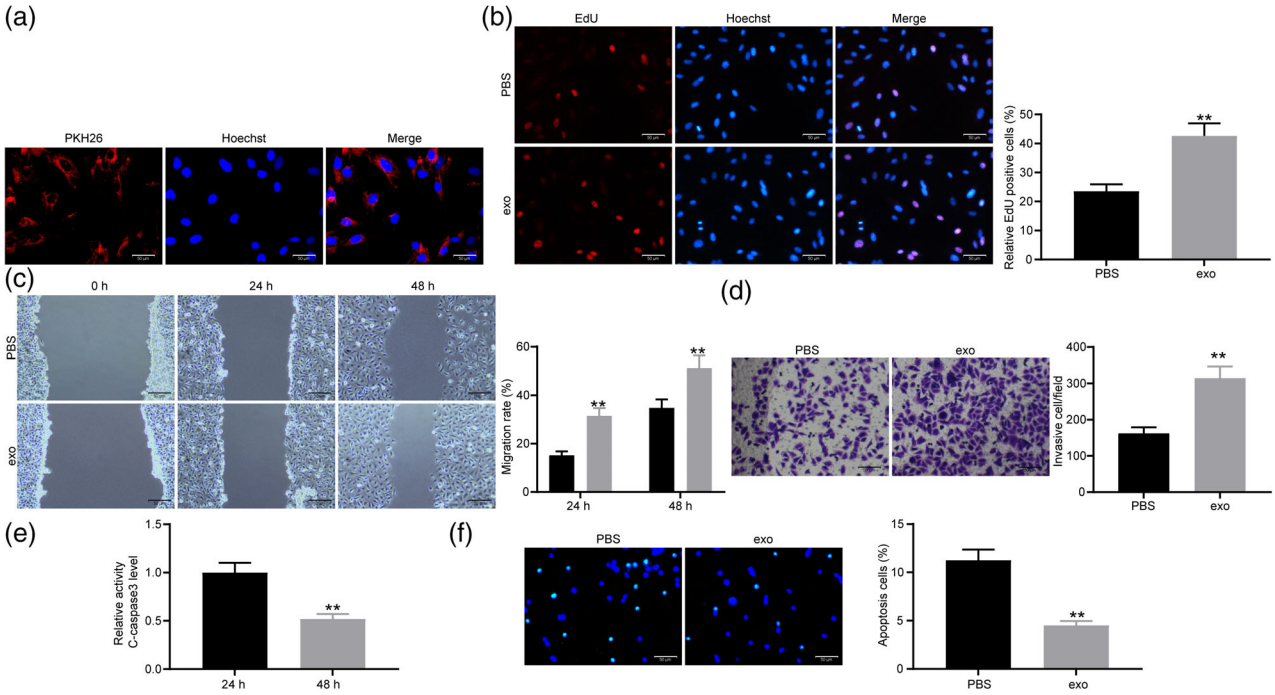

Figure 2 Exosomes inhibit the occurrence of PE. (a) The exosomes in HTR-8/Svneo cells were observed by an inverted microscope. (b) Cell proliferation in HTR-8/Svneo cells treated with PBS and exosomes detected by EdU assay (unpaired *t*-test, $^{**}P < 0.01$). (c) Cell migration in HTR-8/Svneo cells treated with PBS and exosomes detected by wound healing assay (two-way ANOVA, $^{**}P < 0.01$). (d) Cell invasion in HTR-8/Svneo cells treated with PBS and exosomes detected by Transwell assay (unpaired *t*-test, $^{**}P < 0.01$). ■, PBS. ■, exo. (e) Activity of c-caspase 3 detected by c-caspase 3 Kit (unpaired *t*-test, $^{**}P < 0.01$). (f) Cell apoptosis rate detected by TUNEL staining (unpaired *t*-test, $^{**}P < 0.01$).

grew calcified nodules, which contained a small amount of mineral deposits, implying that they had the capability to differentiate into osteoblasts (Figure S1c). Lipid deposition appeared in the cells 25 days after adipogenic induction, and lipid droplets became larger gradually, indicating that the cells could differentiate into adipocytes as well (Figure S1d). These experiments proved that the cells were MSC.

The exosomes were acquired to have a circular or elliptical structure under a transmission electron microscope (TEM) (Figure 1a), and the diameter of exosomes was 30–120 nm (Figure 1b). Exosomes were positive for CD63 and HSP70 but negative for calbindin (Figure 1c). Experiments identified that we have obtained the exosomes from MSC.

The protective effect of exosomes on trophoblasts

The exosomes secreted from MSC marked with PKH26 were perceived under an inverted microscope (Figure 2a). We found that HTR-8/Svneo cells obviously phagocytosed exosomes.

HTR-8/Svneo cells were treated with exosomes with PBS as control. Through the EdU experiment, we found that the positive rate of trophoblasts increased after exosomes treatment (Figure 2b). It was found that exosomes treatment promoted migration and invasion of trophoblasts (Figure 2c–d). The activity of c-caspase-3 was

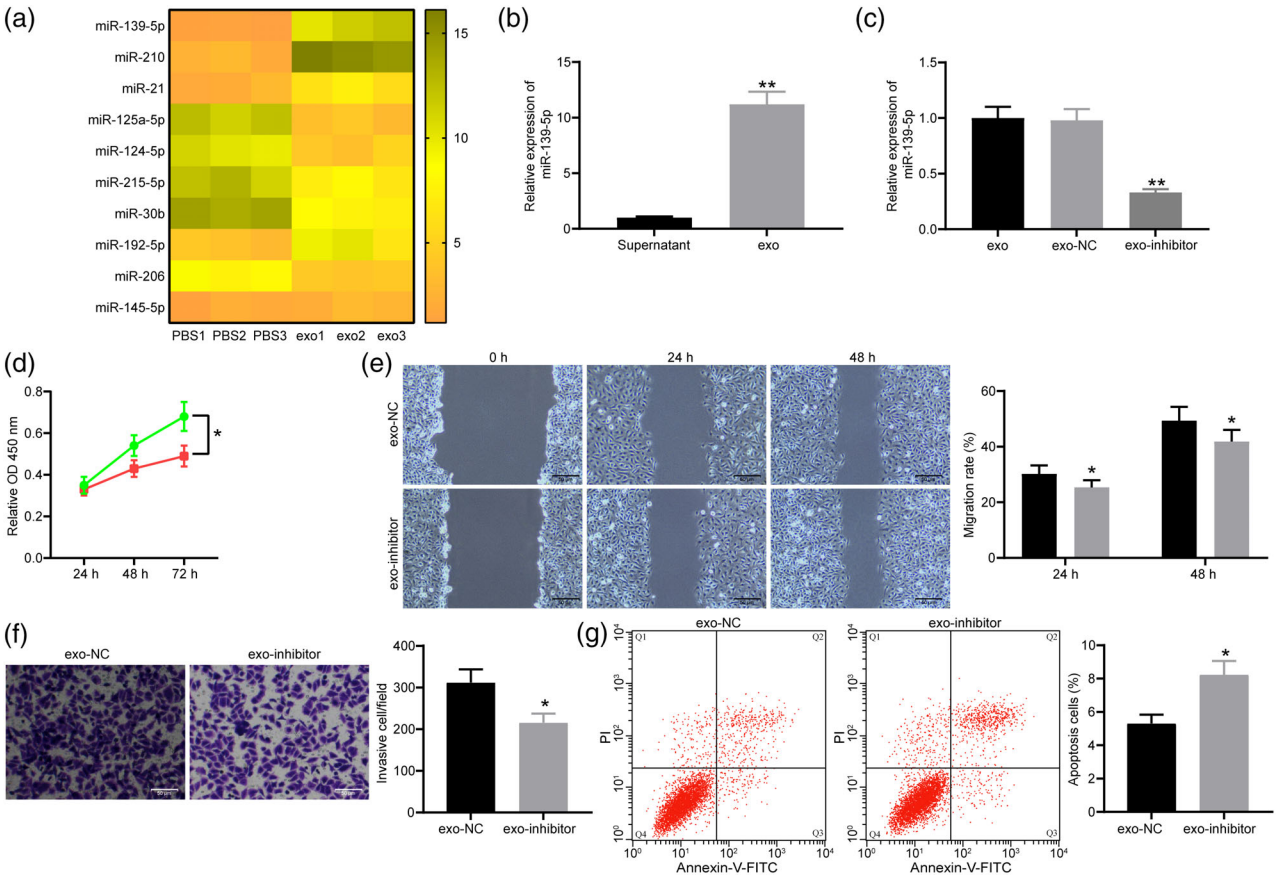

Figure 3 Exosomes exerted its role in PE through the delivery of miR-139-5p. (a) Microarray analysis of the top 10 miRNAs differentially expressed in trophoblasts treated with exosomes. (b) The exosomes significantly enriched miR-139-5p (unpaired *t*-test, $^{**}P < 0.01$). (c) The expression of miR-139-5p in exosomes of hucMSC transfected with miR-139-5p inhibitor measured by RT-qPCR (one-way ANOVA, $^{**}P < 0.01$). (d) Cell proliferation in trophoblasts treated with exo-NC and exo-inhibitor detected by CCK-8 assay (two-way ANOVA, $^{**}P < 0.01$). —● exo-NC. —■ exo-inhibitor. (e) Cell migration in trophoblasts treated with exo-NC and exo-inhibitor detected by wound healing assay (two-way ANOVA, $^{**}P < 0.01$). ■ exo-NC. ■ exo-inhibitor. (f) Cell invasion in trophoblasts treated with exo-NC and exo-inhibitor detected by Transwell assay (unpaired *t*-test, $^{**}P < 0.01$). (g) Cell apoptosis rate of trophoblasts treated with exo-NC and exo-inhibitor detected by TUNEL staining (unpaired *t*-test, $^{**}P < 0.01$).

detected by the c-caspase-3 kit. It was found that exosomes inhibited the activity of c-caspase-3 (Figure 2e). Exosomes hindered apoptosis of trophoblasts (Figure 2f). Above all, exosomes exerted a protective role on trophoblasts.

Exosomes boosted miR-139-5p expression in trophoblasts

The top ten differentially expressed miRNA detected by microarray analysis are presented in Figure 3a. miR-139-5p is the miRNA with the largest difference. It has been previously reported that miR-139-5p promoted the proliferation and invasion of trophoblasts. We thus speculated that exosomes played a role by increasing the expression of miR-139-5p in trophoblasts. The expression of miR-139-5p in the supernatant and the precipitated suspension was measured by RT-qPCR. miR-139-5p was abundant in exosomes (Figure 3b). miR-139-5p inhibitor and its negative control (NC) were transfected into hucMSC to collect exosomes, named exo-inhibitor and exo-NC, respectively. miR-139-5p expression in exosomes of hucMSC transfected with miR-139-5p inhibitor decreased (Figure 3c).

Exo-NC and exo-inhibitor were co-cultured with HTR-8/Svneo cells. CCK-8 assay found that the proliferation ability of trophoblasts transfected with exo-inhibitor decreased significantly (Figure 3d). Trophoblasts treated with exo-inhibitor showed blocked migration and invasion detected by wound healing assay (Figure 3e) and Transwell assay (Figure 3f). Compared trophoblasts treated with exo-NC, the apoptosis rate of trophoblasts co-cultured with exo-inhibitor increased significantly (Figure 3g).

Exosomes inhibited PTEN expression and promoted ERK/MMP-2 pathway activation through miR-139-5p

Starbase (http://starbase.sysu.edu.cn/) predicts that miR-139-5p targets PTEN (Figure 4a). Therefore, we predicted that exosomes could inhibit PTEN expression by increasing the expression of miR-139-5p. miR-139-5p mimic and its control were transfected into HTR-8/Svneo cells, and the effective transfection was detected (Figure 4b). Dual-luciferase reporter gene assay found that miR-139-5p mimic inhibited the activity of WT luciferase (Figure 4c). We found that exosome treatment significantly reduced PTEN expression in trophoblasts (Figure 4d). Further study of the downstream mechanism found that exosomes activated the ERK/MMP-2 pathway through Western blot analysis (Figure 4e).

The ERK/MMP-2 pathway inhibitor blocked the effect of exosomes on trophoblasts

Trophoblasts treated with exosomes were further treated with ERK1/2 inhibitor with trophoblasts treated with exosomes alone as a control. The expression of ERK/MMP-2 pathway-related proteins was measured by Western blot analysis (Figure 5a). ERK1/2 inhibitor successfully inhibited the activation

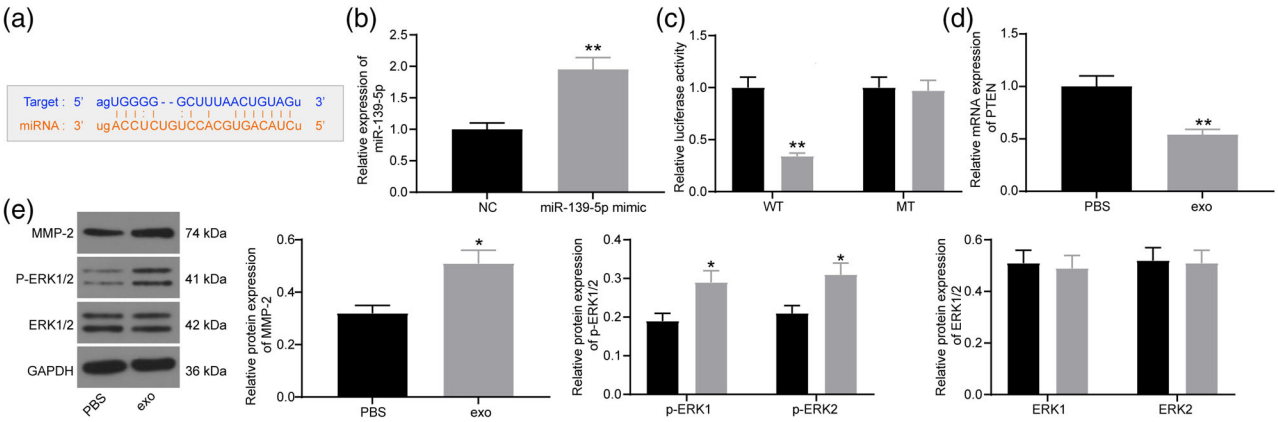

Figure 4 Exosomal miR-139-5p regulated ERK/MMP-2 pathway by interacting with PTEN in trophoblasts. (a) The binding sites between miR-139-5p and PTEN. (b) The transfection efficiency of miR-139-5p mimic detected by RT-qPCR (unpaired *t*-test, $^{**}P < 0.01$). (c) Luciferase activity of cells co-transfected miR-139-5p mimic with WT or MT PTEN (two-way ANOVA, $^{**}P < 0.01$). ■, NC. ■, miR-139-5p-mimic. (d) PTEN expression in exosomes-treated cells by RT-qPCR (unpaired *t*-test, $^{**}P < 0.01$). (e) The protein expression of MMP2 (unpaired *t*-test, $^{*}P < 0.05$) and ERK1/2 (two-way ANOVA, $^{*}P < 0.05$), ■, PBS, ■, exo, as well as the extent of ERK1/2 phosphorylation (two-way ANOVA, $^{*}P < 0.05$) detected by Western blot analysis ■, PBS, ■, exo.

of the ERK1/2 pathway. ERK1/2 inhibitor also repressed the cell proliferation (Figure 5b), migration and invasion (Figure 5c–d) of cells after exosome treatment. By contrast, the ERK1/2 inhibitor promoted the apoptotic rate of cells treated with exosomes identified by flow cytometry (Figure 5e).

Ameliorative effect of exosomes on PE rats

To demonstrate the ameliorative effect of exosomes on PE pathology, we developed a rat model of PE and treated them with exosomes. The timeline of the treatments performed on rats is shown in Figure 6a. Blood pressure was measured in each group of rats every 4 days starting from gestation (Figure 6b). We observed a significant increase in systolic and diastolic blood pressure from day 12 in both PE and PE-exo rats compared to the sham-operated rats, while blood pressure started to decrease significantly in the PE-exo group after exosome treatment and was not significantly different from that of the sham group at day 20. The 24-h proteinuria levels (Figure 6c) of rats were measured on days 15, 17 and 19. We found that PE modeling led to an increase in 24-h proteinuria compared to the sham-operated rats, while 24-h proteinuria was significantly reduced after exosome injections. RT-qPCR experiments were performed on rat placental tissues to detect the expression of related genes (Figure 6d). We found that the expression of miR-139-3p was significantly decreased in the PE rats compared to the sham-operated rats, whereas the expression of PTEN and MMP-2 was significantly increased. The expression of miR-139-3p in rat placental tissues was significantly restored and the expression of PETN and MMP-2 was significantly reduced

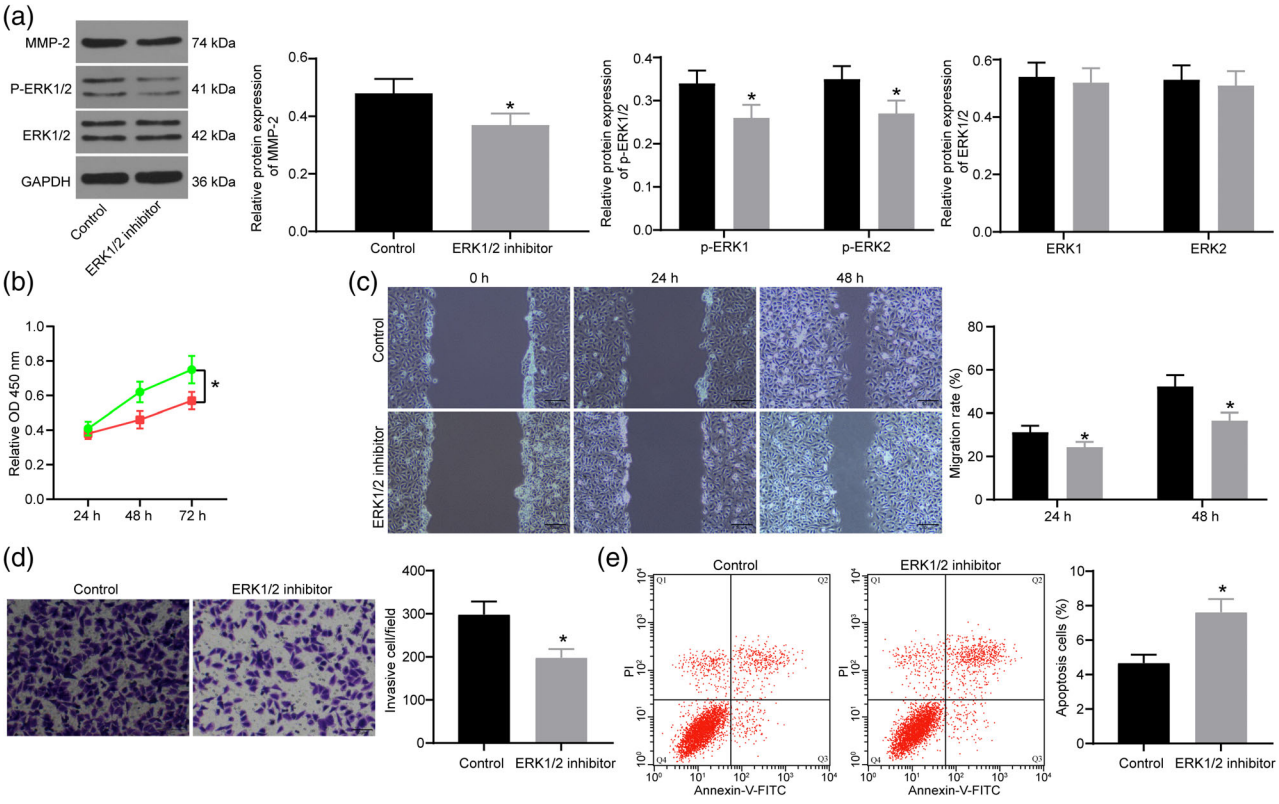

Figure 5 Inhibition of ERK/MMP-2 pathway reverses the role of exosomes on trophoblasts. (a) The protein expression of MMP2 (unpaired *t*-test, $*P < 0.05$) and ERK1/2 (two-way ANOVA, $*P < 0.05$), ■, control, ■, ERK 1/2 inhibitor, as well as the extent of ERK1/2 phosphorylation (two-way ANOVA, $*P < 0.05$), ■, control. ■, ERK 1/2 inhibitor, detected by Western blot analysis. (b) Proliferation of trophoblasts treated with exosomes and ERK1/2 inhibitor measured by CCK-8 assay (two-way ANOVA, $*P < 0.05$). —●—, control. —■—, ERK 1/2 inhibitor. (c) Migration of trophoblasts treated with exosomes and ERK1/2 inhibitor measured by wound healing assay (two-way ANOVA, $*P < 0.05$). ■, control. ■, ERK 1/2 inhibitor. (d) Invasion of trophoblasts treated with exosomes and ERK1/2 inhibitor measured by Transwell assay (unpaired *t*-test, $*P < 0.05$). (e) Apoptosis of trophoblasts treated with exosomes and ERK1/2 inhibitor measured by flow cytometry (unpaired *t*-test, $*P < 0.05$).

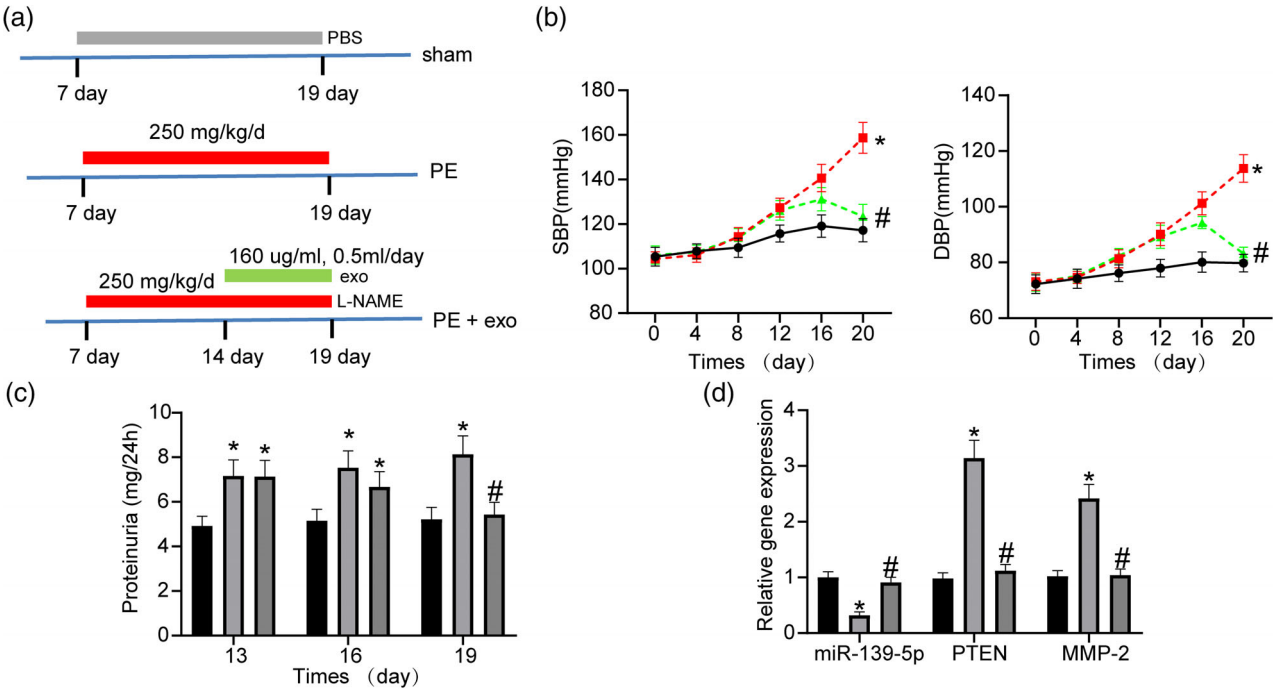

Figure 6 Ameliorating effect of exosomes on pathology in PE rats. (a) Time course of treatment for pregnant rats. (b) Changes in blood pressure in pregnant rats (two-way ANOVA, $^{*}P < 0.05$, $^{\#}P < 0.05$) (*left*: —●—, sham. --■--, PE. --▲--, PE + exo; *right*: —●—, sham. --■--, PE. --▲--, PE + exo). (c) 24-h proteinuria in each group of rats on the indicated days (two-way ANOVA, $^{*}P < 0.05$, $^{\#}P < 0.05$). ■, sham. ▭, PE. ▭, PE + exo. (d) Expression of miR-139-5p, PTEN and MMP2 in the placenta of rats assessed by RT-qPCR (two-way ANOVA, $^{*}P < 0.05$, $^{\#}P < 0.05$). ■, sham. ▭, PE. ▭, PE + exo.

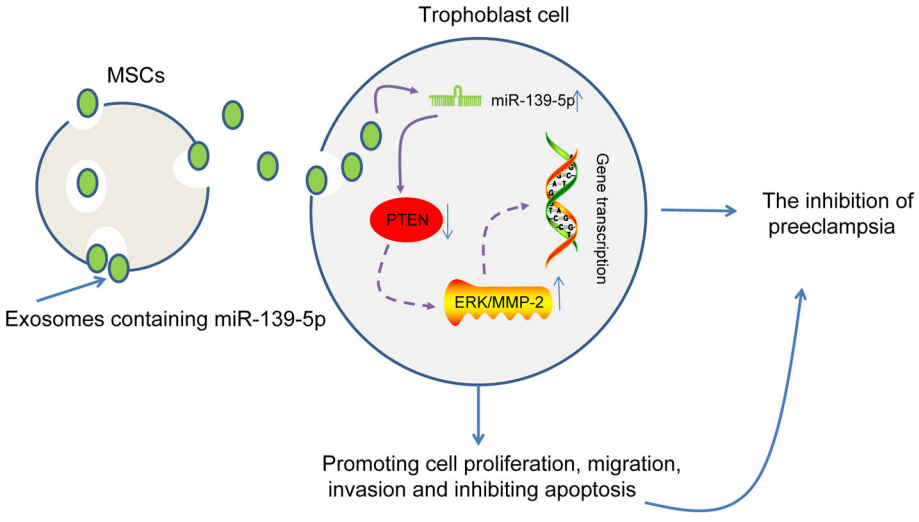

Figure 7 Possible mechanism of exosomes in PE. The exosomal miR-139-5p derived from hucMSC promotes the trophoblast proliferation, migration and invasion and inhibits apoptosis by down-regulation of PTEN and activation of the ERK/MMP-2 pathway to inhibit the occurrence of PE.

after exosome treatment. Through *in vivo* experiments, we demonstrated that exosome therapy significantly improved the pathological changes such as hypertension and proteinuria caused by PE.

Discussion

PE is related to diminished fetal trophoblast cell invasion and damaged maternal spiral vein remodeling,

which causes disfavored uterine placental perfusion.[8] MiRNA were found to interact with mRNA and signaling pathways to regulate biological processes of PE.[22,23] Our study searched the function of hucMSC-secreted exosomal miR-139-5p as well as the downstream PTEN and ERK/MMP-2 pathway in trophoblasts. The results revealed that hucMSC-secreted exosomal miR-139-5p and inhibition of PTEN regulated trophoblast activities by regulating the ERK/MMP-2 pathway (Figure 7).

We initially uncovered that exosomes foster the migration and invasion and restrain apoptosis of trophoblasts, and exosomes act through the delivery of miR-139-5p. Pregnancy-related and trophoblast-originated exosomes might exert vital regulatory influences on the intracellular target cells and regulate the maintenance and decisive success of pregnancy.[24] In addition, exosomes released by hucMSC improved the morphology of placental tissue in rats with PE by hampering cell apoptosis and promoting angiogenesis in placental tissue,[21] indicating the impact of exosome on the pathogenesis of PE. MSC-originated exosomes overexpressing H19 reduced let-7b and strengthened forkhead box protein O1 (FOXO1) expression to trigger the protein kinase B (AKT) pathway, thus enhancing trophoblast activities.[8] A report summarized the exo-miRNA of umbilical cord blood in healthy and PE pregnant females systematically and validated that miR-125a-5p dysregulation might influence HTR8/SVneo cell angiogenesis, which is an indicative of miR-125a-5p involvement throughout PE progression.[10] Placenta-connected serum exosomes could constrain expression of endothelial nitric oxide synthase during PE progression in endothelial cells, and this occurrence may be fairly caused by raised miR-155 expression in the exosomes.[25] Besides, MSC-derived exosomal miR-146a-5p and miR-548e-5p possess anti-inflammatory capability on human trophoblasts and were suggested to be innovative targets for healing inflammatory-associated diseases during pregnancy, such as PE.[26] Exosomal hsa-miR-210, actively produced from the trophoblasts in PE, are involved in PE etiology by intercellular communication.[27] In the current investigation, we employed microarray analysis to screen out the top 10 differentially expressed miRNAs in exosome-treated trophoblasts, among which miR-139-5p was revealed to be the most significantly expressed one (Fold change ≈ 9). miR-139-5p has been indicated to mediate the expression of peripheral myelin protein 22 to block cell growth and proliferation by governing the nuclear factor-κB signaling pathway in gastric cancer.[28] Interestingly, it has been proposed that mice treated with exosomes extracted from patients with depression presented depressive-like behaviors, which was connected with miR-139-5p-controlled neurogenesis.[29] Extracellular miRNAs circulating at the second trimester in parental blood are linked with fetal development, and miR-139-5p was associated with weight-for-gestational age z-score.[30] In addition, there was also a study, showing that miR-139-5p expression was declined in PE patients and miR-139-5p stimulated the trophoblast invasion and proliferation.[15] Our rescue experiments provided evidence that miR-139-5p inhibitor abrogated the promotive role of exosomes on trophoblast invasion and proliferation, implying that hucMSC-exosomes functioned in trophoblasts via delivering miR-139-5p.

Another critical conclusion was that exosomal miR-139-5p could downregulate PTEN and trigger the ERK/MMP-2 pathway. It was stated that PTEN was strongly connected to various tumors, including breast, endometrial and esophageal squamous cell carcinomas.[31–33] More specifically, PTEN was also found to play a part in trophoblast cell proliferation and PE development regulated by long noncoding RNA T cell leukemia/lymphoma 6.[34] Moreover, strengthened PTEN in HTR-8/SVneo cells displayed partial degeneration of the improved cell infiltration prompted by miR-21.[35] PTEN could also be targeted by miR-144 so as to control the activities of trophoblasts in PE.[36] In the current study, microarray analysis and dual-luciferase reporter gene assay displayed that miR-139-5p was able to mediate PTEN negatively. Through triggering the MEK1/ERK pathway, PTEN silencing could hinder the oxidative stress injury and apoptosis in hippocampal cells in infant rats caused by Sevoflurane.[37] Avermectin regulated the PI3K-ERK pathway negatively to reduce respiratory burst in carp by activating PTEN demethylation.[38] Down-regulation of a trophoblast-derived MMP-9, and the main protein hydrolase ERK/MMP-2 pathways could lead to invasion disorders of trophoblasts in the PE placenta.[39] Through constraining the ERK/MMP-2 pathway, miR-517-5p, which is highly expressed in PE placenta, could stimulate invasive and proliferative capabilities of JAR cells(a √choriocarcinoma cell line).[40] Intriguingly, miR-139-5p inhibited MMP2 expression through direct targeting in non-small-cell lung cancer cells.[41] Collectively, we established in the current study that hucMSC-secreted exosomal miR-139-5p enhanced trophoblast activity by activating the ERK/MMP-2 pathway via PTEN inhibition. Even though this study

underscored the beneficial effect of exosomes derived from hucMSC in PE rats, the application of exosomes in clinical treatment warrants further investigation and confirmation.

Disclosure

None declared.

References

1. Belay Tolu L, Yigezu E, Urgie T, Feyissa GT. Maternal and perinatal outcome of preeclampsia without severe feature among pregnant women managed at a tertiary referral hospital in urban Ethiopia. *PLoS One* 2020; **15**: e0230638.
2. Rahman RA, Murthi P, Singh H *et al*. Hydroxychloroquine mitigates the production of 8-Isoprostane and improves vascular dysfunction: Implications for treating preeclampsia. *Int J Mol Sci* 2020; **21**: 2504.
3. Turanov AA, Lo A, Hassler MR *et al*. RNAi modulation of placental sFLT1 for the treatment of preeclampsia. *Nat Biotechnol* 2018; **36**: 1164–1173.
4. Feng H, Wang L, Zhang G, Zhang Z, Guo W. Oxidative stress activated by Keap-1/Nrf2 signaling pathway in pathogenesis of preeclampsia. *Int J Clin Exp Pathol* 2020; **13**: 382–392.
5. Xue P, Fan W, Diao Z *et al*. Up-regulation of PTEN via LPS/AP-1/NF-kappaB pathway inhibits trophoblast invasion contributing to preeclampsia. *Mol Immunol* 2020; **118**: 182–190.
6. Jena MK, Sharma NR, Petitt M, Maulik D, Nayak NR. Pathogenesis of preeclampsia and therapeutic approaches targeting the placenta. *Biomolecules* 2020; **10**: 953.
7. Basmaeil YS, Algudiri D, Alenzi R, Al Subayyil A, Alaiya A, Khatlani T. HMOX1 is partly responsible for phenotypic and functional abnormalities in mesenchymal stem cells/stromal cells from placenta of preeclampsia (PE) patients. *Stem Cell Res Ther* 2020; **11**: 30.
8. Chen Y, Ding H, Wei M *et al*. MSC-secreted Exosomal H19 promotes Trophoblast cell invasion and migration by Downregulating let-7b and Upregulating FOXO1. *Mol Ther Nucleic Acids* 2020; **19**: 1237–1249.
9. Salomon C, Guanzon D, Scholz-Romero K *et al*. Placental exosomes as early biomarker of preeclampsia: Potential role of exosomal microRNAs across gestation. *J Clin Endocrinol Metab* 2017; **102**: 3182–3194.
10. Xueya Z, Yamei L, Sha C *et al*. Exosomal encapsulation of miR-125a-5p inhibited trophoblast cell migration and proliferation by regulating the expression of VEGFA in preeclampsia. *Biochem Biophys Res Commun* 2020; **525**: 646–653.
11. Adhami M, Haghdoost AA, Sadeghi B, Malekpour AR. Candidate miRNAs in human breast cancer biomarkers: A systematic review. *Breast Cancer* 2018; **25**: 198–205.
12. Gu SQ, Luo JH, Yao WX. The regulation of miR-139-5p on the biological characteristics of breast cancer cells by targeting COL11A1. *Math Biosci Eng* 2019; **17**: 1428–1441.
13. Xiu D, Liu L, Cheng M, Sun X, Ma X. Knockdown of lncRNA TUG1 enhances radiosensitivity of prostate cancer via the TUG1/miR-139-5p/SMC1A axis. *Onco Targets Ther* 2020; **13**: 2319–2331.
14. Zhang Z, Li W, Jiang D, Liu C, Lai Z. MicroRNA-139-5p inhibits cell viability, migration and invasion and suppresses tumor growth by targeting HDGF in non-small cell lung cancer. *Oncol Lett* 2020; **19**: 1806–1814.
15. Huang J, Zheng L, Kong H, Wang F, Su Y, Xin H. miR-139-5p promotes the proliferation and invasion of trophoblast cells by targeting sFlt-1 in preeclampsia. *Placenta* 2020; **92**: 37–43.
16. Liu W, Yang D, Chen L *et al*. Plasma exosomal miRNA-139-3p is a novel biomarker of colorectal cancer. *J Cancer* 2020; **11**: 4899–4906.
17. Li H, Ouyang Y, Sadovsky E, Parks WT, Chu T, Sadovsky Y. Unique microRNA signals in plasma exosomes from pregnancies complicated by preeclampsia. *Hypertension* 2020; **75**: 762–771.
18. Maduray K, Moodley J, Mackraj I. The impact of circulating exosomes derived from early and late onset pre-eclamptic pregnancies on inflammatory cytokine secretion by BeWo cells. *Eur J Obstet Gynecol Reprod Biol* 2020; **247**: 156–162.
19. Thery C, Amigorena S, Raposo G, Clayton A. Isolation and characterization of exosomes from cell culture supernatants and biological fluids. *Curr Protoc Cell Biol* 2006; **3**: 22.
20. van der Pol E, Coumans FA, Grootemaat AE *et al*. Particle size distribution of exosomes and microvesicles determined by transmission electron microscopy, flow cytometry, nanoparticle tracking analysis, and resistive pulse sensing. *J Thromb Haemost* 2014; **12**: 1182–1192.
21. Xiong ZH, Wei J, Lu MQ, Jin MY, Geng HL. Protective effect of human umbilical cord mesenchymal stem cell exosomes on preserving the morphology and angiogenesis of placenta in rats with preeclampsia. *Biomed Pharmacother* 2018; **105**: 1240–1247.
22. Kang JH, Song H, Yoon JA *et al*. Preeclampsia leads to dysregulation of various signaling pathways in placenta. *J Hypertens* 2011; **29**: 928–936.
23. Mayor-Lynn K, Toloubeydokhti T, Cruz AC, Chegini N. Expression profile of microRNAs and mRNAs in human placentas from pregnancies complicated by preeclampsia and preterm labor. *Reprod Sci* 2011; **18**: 46–56.
24. Stefanski AL, Martinez N, Peterson LK *et al*. Murine trophoblast-derived and pregnancy-associated exosome-enriched extracellular vesicle microRNAs: Implications for placenta driven effects on maternal physiology. *PLoS One* 2019; **14**: e0210675.
25. Shen L, Li Y, Li R *et al*. Placentaassociated serum exosomal miR155 derived from patients with preeclampsia inhibits eNOS expression in human umbilical vein endothelial cells. *Int J Mol Med* 2018; **41**: 1731–1739.
26. Yang C, Lim W, Park J, Park S, You S, Song G. Anti-inflammatory effects of mesenchymal stem cell-derived exosomal microRNA-146a-5p and microRNA-548e-5p on human trophoblast cells. *Mol Hum Reprod* 2019; **25**: 755–771.
27. Biro O, Fothi A, Alasztics B, Nagy B, Orban TI, Rigo J Jr. Circulating exosomal and Argonaute-bound microRNAs in preeclampsia. *Gene* 2019; **692**: 138–144.
28. Hou J, Zhuo H, Chen X *et al*. MiR-139-5p negatively regulates PMP22 to repress cell proliferation by targeting the NF-kappaB signaling pathway in gastric cancer. *Int J Biol Sci* 2020; **16**: 1218–1229.

29. Wei ZX, Xie GJ, Mao X *et al*. Exosomes from patients with major depression cause depressive-like behaviors in mice with involvement of miR-139-5p-regulated neurogenesis. *Neuropsychopharmacology* 2020; **45**: 1050–1058.
30. Rodosthenous RS, Burris HH, Sanders AP *et al*. Second trimester extracellular microRNAs in maternal blood and fetal growth: An exploratory study. *Epigenetics* 2017; **12**: 804–810.
31. El Abbass KA, Abdellateif MS, Gawish AM, Zekri AN, Malash I, Bahnassy AA. The role of breast cancer stem cells and some related molecular biomarkers in metastatic and nonmetastatic breast cancer. *Clin Breast Cancer* 2020; **20**: e373–e384.
32. Liang G, Wang H, Shi H *et al*. Porphyromonas gingivalis promotes the proliferation and migration of esophageal squamous cell carcinoma through the miR-194/GRHL3/PTEN/Akt axis. *ACS Infect Dis* 2020; **6**: 871–881.
33. Wang QA, Yang Y, Liang X. LncRNA CTBP1-AS2 sponges miR-216a to upregulate PTEN and suppress endometrial cancer cell invasion and migration. *J Ovarian Res* 2020; **13**: 37.
34. Wu JL, Wang YG, Gao GM, Feng L, Guo N, Zhang CX. Overexpression of lncRNA TCL6 promotes preeclampsia progression by regulating PTEN. *Eur Rev Med Pharmacol Sci* 2019; **23**: 4066–4072.
35. Lou CX, Zhou XT, Tian QC, Xie HQ, Zhang JY. Low expression of microRNA-21 inhibits trophoblast cell infiltration through targeting PTEN. *Eur Rev Med Pharmacol Sci* 2018; **22**: 6181–6189.
36. Xiao J, Tao T, Yin Y, Zhao L, Yang L, Hu L. miR-144 may regulate the proliferation, migration and invasion of trophoblastic cells through targeting PTEN in preeclampsia. *Biomed Pharmacother* 2017; **94**: 341–353.
37. Liu T, Dong X, Wang B *et al*. Silencing of PTEN inhibits the oxidative stress damage and hippocampal cell apoptosis induced by Sevoflurane through activating MEK1/ERK signaling pathway in infant rats. *Cell Cycle* 2020; **19**: 684–696.
38. Zheng S, Wang S, Zhang Q, Zhang Z, Xu S. Avermectin inhibits neutrophil extracellular traps release by activating PTEN demethylation to negatively regulate the PI3K-ERK pathway and reducing respiratory burst in carp. *J Hazard Mater* 2020; **389**: 121885.
39. Wei J, Fu Y, Mao X, Jing Y, Guo J, Ye Y. Decreased Filamin b expression regulates trophoblastic cells invasion through ERK/MMP-9 pathway in pre-eclampsia. *Ginekol Pol* 2019; **90**: 39–45.
40. Fu JY, Xiao YP, Ren CL *et al*. Up-regulation of miR-517-5p inhibits ERK/MMP-2 pathway: Potential role in preeclampsia. *Eur Rev Med Pharmacol Sci* 2018; **22**: 6599–6608.
41. Zeng F, Yu N, Han Y, Ainiwaer J. The long non-coding RNA MIAT/miR-139-5p/MMP2 axis regulates cell migration and invasion in non-small-cell lung cancer. *J Biosci* 2020; **45**: 51

Supporting information

Additional Supporting Information may be found in the online version of this article at the publisher's web-site:

Appendix S1: Supporting information

Figure S1: Characterization of MSC. (a) Morphological observation of MSC. (b) Identification of surface indicators of MSC by means of flow cytometry. (c) Osteogenic differentiation assessed by alizarin red staining. (d) Adipogenic differentiation assessed by oil red O staining.

